Boundary lubrication of oxide surfaces by Poly(L-lysine)-*g*-poly(ethylene glycol) (PLL-*g*-PEG) in aqueous media

Seunghwan Lee[a], Markus Müller[a], Monica Ratoi-Salagean[b], Janos Vörös[a], Stéphanie Pasche[a], Susan M. De Paul[a], Hugh A. Spikes[b], Marcus Textor[a], and Nicholas D. Spencer[a,*]

[a]*Laboratory for Surface Science and Technology, Department of Materials, ETH-Zürich, Sonneggstrasse 5, Zürich, CH-8092, Switzerland*
[b]*Tribology Section, Department of Mechanical Engineering, Imperial College, London, SW7 2BX U.K.*

Received 15 December 2002; accepted 10 March 2003

In this work, we have explored the application of poly(L-lysine)-*g*-poly(ethylene glycol) (PLL-*g*-PEG) as an additive to improve the lubricating properties of water for metal-oxide-based tribo-systems. The adsorption behavior of the polymer onto both silicon oxide and iron oxide has been characterized by optical waveguide lightmode spectroscopy (OWLS). Several tribological approaches, including ultra-thin-film interferometry, the mini traction machine (MTM), and pin-on-disk tribometry, have been employed to characterize the frictional properties of the oxide tribo-systems in various contact regimes. The polymer appears to form a protective layer on the tribological interface in aqueous buffer solution and improves both the load-carrying and boundary-layer-lubrication properties of water.

KEY WORDS: poly(L-lysine)-*g*-poly(ethylene glycol) (PLL-*g*-PEG), aqueous lubrication, boundary lubrication

1. Introduction

Water possesses several characteristics that are desirable for its use as a lubricant, such as being environmentally friendly, advantageous for heat management and economical. Synovial joints, such as hip, knee, shoulder, ankle and finger joints, can display friction coefficients, μ, that are less than 0.003 [1–4]. However, extremely low friction in natural joint systems cannot be achieved by water alone, due to its inability to form useful boundary films and its extremely low pressure-coefficient of viscosity [1–4]. The latter has serious consequences for elastohydrodynamic lubrication with water and thus limits the load-carrying capacity of water-lubricated tribo-systems. Nature deals with these issues by using "smart", pressure-responsive cartilage surfaces as sliding partners [4]. In efforts to use water as a lubricant in engineering systems, several approaches are employed to modify the lubricating properties of water, including oil-in-water (O/W) emulsions [5–7] or aqueous surfactants [8–11]. In both approaches, the formation of a protective film, either instantaneously or irreversibly, is known to be responsible for a lubrication effect.

In recent years, some attention has been paid to end-grafted polymers that exhibit unique tribological properties in organic media [12–18]. In "good" solvents, end-grafted polymers are strongly stretched and keep the polymer-bearing interfaces apart during sliding, while maintaining a relatively fluid layer at the interface. This mechanism strongly contrasts with the sliding of a rigid interface where surfaces are brought into close contact and the solvent molecules squeezed out during sliding. Coefficients of friction as low as 0.001 have been observed under light compression of polymer-grafted interfaces, although higher friction forces were observed in a higher-pressure regime [13,14]. These observations hint that brush-like polymers may provide an alternative approach for improving the lubrication properties in an aqueous environment, providing that their chemical and structural properties are properly designed.

We employed poly(L-lysine)-*g*-poly(ethylene glycol) (PLL-*g*-PEG) as an additive to improve the lubricating properties of water for metal-oxide-based tribo-systems. PLL-*g*-PEG has been extensively investigated in previous studies for use in a wide array of biomedical applications [19–23]. As shown in figure 1, this co-polymer is composed of a polycationic PLL backbone and a non-reactive PEG side chain. The PLL backbone is positively charged at pH $\leq$ 10 due to protonation of the primary amine groups, and readily adsorbs onto a negatively charged surface, mainly through electrostatic interactions. Many metal oxide surfaces display isoelectric points (IEP) that lie below pH 10 [24], and thus can be effectively coated by this polyelectrolyte in aqueous conditions. Some of the NH_2 functional groups of the PLL are used for coupling PEG side-chains, thus resulting in hydrophilic, flexible, brush-like side chains.

In this work, we explore the potential use of PLL-*g*-PEG as an additive to improve the lubrication properties of water for tribo-systems composed of metal

*To whom correspondence should be addressed. E-mail: nspencer@surface.mat.ethz.ch

1023-8883/03/1000–0231/0

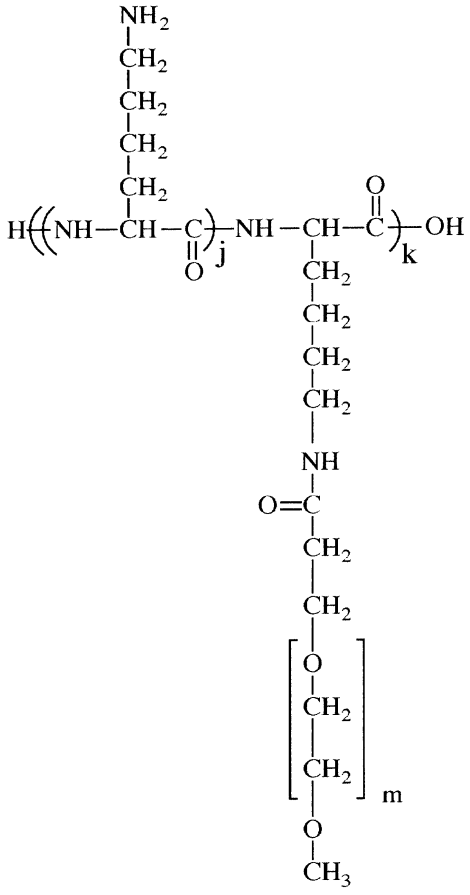

Figure 1. A schematic illustration of PLL-*g*-PEG.

oxides. For this purpose, several macroscopic tribological approaches, including ultra-thin film interferometry, the mini traction machine (MTM), and pin-on-disk tribometry, representing a pure rolling, mixed sliding/rolling, and pure sliding respectively, all in a non-conformal sphere-on-plane geometry, have been employed.

2. Materials and methods

2.1. PLL(10)-g[2.9]-PEG(2)

PLL(10)-*g*[2.9]-PEG(2) denotes a graft co-polymer with a PLL backbone of molecular weight 10 kDa, a grafting ratio of (lysine-mer)/(PEG side chains) of 2.9, and a PEG molecular weight 2 kDa.

The PLL-*g*-PEG co-polymer has been synthesized according to a method described in previous publications [22,23]. Briefly, poly(L-lysine) hydrobromide (16 kDa including HBr, Sigma, St. Louis, MO, USA) was dissolved at a concentration of 100 mM in sodium borate buffer solution (50 mM) adjusted to pH 8.5. The solution was filter sterilized (0.22 μm pore-size filter). For the grafting of PEG onto PLL, the *N*-hydroxysuccinimidyl ester of methoxypoly(ethylene glycol) propionic acid (mol. wt. 2 kDa, mPEG-SPA, Shearwater Corporation, Huntsville, AL, USA) was added to PLL solution. The reaction was allowed to proceed for 6 h at room temperature, after which the reaction mixture was dialyzed (Spectra-Por, mol. wt. cutoff size 6–8 kDa, Spectrum, Houston, TX, USA) for 48 h against deionized water. The product was freeze-dried and stored at $-20\,^{\circ}$C. Detailed analytical information of the product produced using this method is available in previous publications [22,23].

The PLL(10)-*g*[2.9]-PEG(2) was dissolved in 10 mM HEPES (4-(2-hydroxyethyl)piperazine-1-ethanesulfonic acid (Sigma, St. Louis, MO, USA), adjusted to pH 7.4 with 1.0 M NaOH solution) with a concentration of 0.25 mg/ml and this solution was used for all subsequent experiments. For cases where the comparison of the PLL(10)-*g*[2.9]-PEG(2) with PLL(10) alone is needed, PLL(10) solution was prepared by dissolving the poly(L-lysine) hydrobromide (mol. wt. 16 kDa including HBr, Sigma, St. Louis, MO, USA) in 10 mM HEPES with a concentration of 0.045 mg/ml to maintain the concentration of PLL constant in both PLL and PLL-*g*-PEG experiments.

2.2. Optical waveguides lightmode spectroscopy (OWLS)

Optical Waveguide Lightmode Spectroscopy (OWLS) was employed to investigate the adsorption behavior of the polymers on the tribo-pair surfaces. OWLS is based on grating-assisted in-coupling of a He-Ne laser into a planar waveguide, and allows the direct online monitoring of macromolecule adsorption. This method is highly sensitive up to a distance of 100 nm above the surface of the waveguide (sensitivity limit, $\sim$1 ng/cm^2). Furthermore, a measurement-time resolution of 3 s allows for the *in situ*, real-time study of adsorption kinetics. The waveguide chips used for OWLS measurements were purchased from MicroVacuum Ltd. (Budapest, Hungary) and consisted of a 1-mm-thick AF 45 glass substrate and a 200-nm-thick $Si_{0.75}Ti_{0.25}O_2$ waveguiding layer at the surface. A silicon oxide (ca. 12 nm) or iron oxide layer (ca. 1 nm) was sputter coated on top of the waveguiding layer in a Leybold dc-magnetron Z600 sputtering unit. The coating conditions and the principles of OWLS investigations have been described in detail elsewhere [25–27].

All OWLS experiments were carried out in a BIOS-I instrument (ASI AG, Zürich, Switzerland) using a Kalrez (Dupont, Wilmington, DE, USA) flow-through cell ($8 \times 2 \times 1$ mm) [25]. The solution exchange was carried out by syringe injection (1 ml within 10 s). Adsorbed mass density data were calculated according to de Feijter's formula from the adsorbed layer thickness and refractive index values from the mode equations [28]. A refractive index increment (dn/dc) value of 0.169 cm^3/g, as determined in a refractometer (Carl

Zeiss, Jena, Germany), was used for the calculation of PLL(10)-*g*[2.9]-PEG(2) adsorption.

2.3. Ultra-thin film interferometry

Ultra-thin film interferometry is a unique approach to measuring the film thickness under a lubricated contact [29]. The set-up is schematically illustrated in figure 2. A lubricated contact is formed between a loaded steel ball and the flat surface of a glass disk. The disk is driven with respect to the nominal axis in contact with the ball and thus can drive the ball in pure rolling contact. The surface of the glass disk is coated, first with a very thin, semi-reflecting layer of chromium, on top of which is a 400-nm layer of transparent silica, as a spacer layer. Thus, the ultra-thin film interferometry tribo-pair in this work represents an FeO_x/SiO_x interface. White light is shone through the glass into the contact, where a proportion is reflected back from the chromium layer while the remainder passes through the silica layer and the polymer-containing water before being reflected from the steel ball surface. Since the two beams have traveled different distances, they interfere at wavelengths that depend on the path difference, i.e. on the sum of silica and lubricant film thickness. The interference pattern from the contact is passed to a spectrometer and the resultant dispersed light analyzed to determine the precise wavelength of maximum constructive interference from the center of the contact. This yields an accurate measure of the composite film thickness, from which the spacer layer can be subtracted.

The refractive index of the lubricant solution is a necessary input for the calculation of the film thickness. The refractive index of the polymer-containing buffer solution is expected to be different from that of pure water (1.33) for two reasons. Firstly, addition of polymers into water results in an increase of the refractive index of the lubricant solution, which was already described in section 2.2. The same incremental value of $0.169\,cm^3/g$ (dn/dc) was considered here. Secondly, the increased pressure at the contact point also results in an increase of the refractive index of the lubricant solution. However, in previous studies, measurement by two-angle interferometry showed that an increase in pressure from atmospheric to 1 GPa alters the refractive index of oil by less than 10% [29–31]. We assume that this is applicable to polymer solutions as well. The refractive index of the polymer solutions is thus calculated to lie between 1.34 (negligible pressure effect) and 1.47 (10% increase by pressure effect). As a compromise, a refractive index of 1.4 has been used for the calculation. As the film thickness is inversely proportional to the refractive index [29], the uncertainty of the film thickness in this work corresponds to ±5%.

All the measurements were carried out under a fixed load (20.0 N) and temperature (~25 °C) and along the same track of the disk. The radii of the ball and disk tracks are 9.5 and 17.75 mm, respectively. The roughness values (R_a) of the ball and disk tracks are 11 and 5 nm respectively. For smooth surface contact, the maximum contact pressure in this configuration is, according to Hertz equations, 0.51 GPa (see table 1). The separation of the surfaces by a thin lubricating film will not significantly change this pressure. In practice, however, because of the finite roughness of the surfaces, there will be local variations from the Hertz pressure distribution at an asperity scale. A thin boundary or EHL film may significantly reduce these variations.

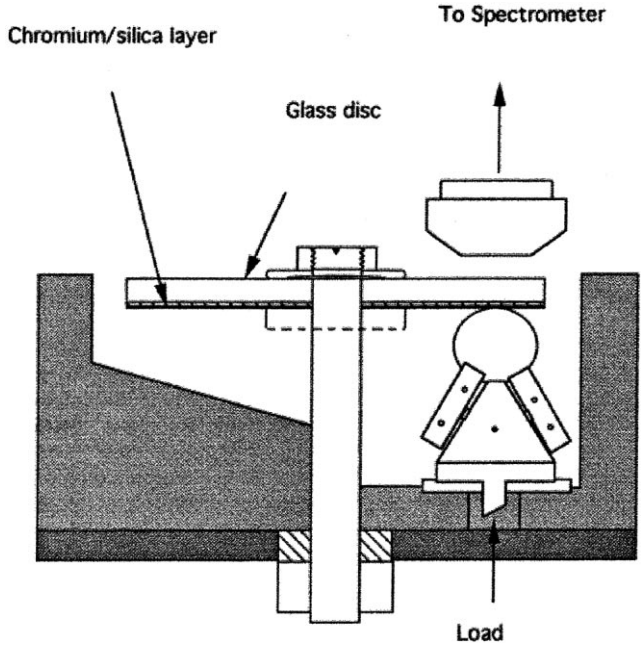

Figure 2. A schematic set-up of ultra-thin film interferometry.

2.4. Mini traction machine (MTM)

A mini traction machine (MTM, PCS Instruments, London, U.K.) was employed to characterize the lubrication properties of the polymers in a mixed sliding/rolling contact regime. The set-up of the instrument is schematically illustrated in figure 3. A lubricated contact is formed between a polished steel ball and a flat steel surface, thus representing an FeO_x/FeO_x interface. In contrast to the other instruments employed in this work, which provide either a pure rolling contact (ultra-thin film interferometry, section 2.3) or a pure sliding contact (pin-on-disk tribometer, section 2.5), MTM provides a mixed sliding/rolling contact through the independent control of the ball and disk velocities. The slide/roll ratio, SRR, is defined as the percentage ratio of the *difference* and the *mean* of the ball velocity (u_{ball}) and disk velocity (u_{disk}), i.e.

$$SRR = \frac{|u_{ball} - u_{disk}|}{\left(\frac{u_{ball} + u_{disk}}{2}\right)} \times 100\%.$$

Table 1
The calculated maximum contact pressure (Hertzian) for the configuration (sphere on plane) used in this work (maximum contact pressure, $P_0 = 1/\pi \cdot \sqrt[3]{6WE^{*2}/R^2}$ where W = load, R = radius of the balls and $E^* = \left((1-\nu_1^2)/E_1 + (1-\nu_2^2)/E_2\right)^{-1}$ where E_1 and ν_1 are Young's modulus and Poisson ratio of the ball and E_2 and ν_2 are Young's modulus and the Poisson ratio of the disk respectively. $E_{steel} = 203$ GPa, $E_{silica} = 72$ GPa, $\nu_{steel} = 0.3$ and $\nu_{silica} = 0.2$ [32]).

Instrument	Tribo-pair (sphere/plane)	R	W	P_0
Ultra-thin film interferometry	silica/steel	9.5 mm	20.0 N	0.51 GPa
MTM	steel/steel	9.5 mm	3.0 N	0.04 GPa
	steel/steel	9.5 mm	20.0 N	0.81 GPa
Pin-on-disk	silica glass/steel	3 mm	0.5 N	0.32 GPa
	silica glass/steel	3 mm	1.0 N	0.41 GPa
	silica glass/steel	3 mm	2.0 N	0.51 GPa
	silica glass/steel	3 mm	5.0 N	0.70 GPa
	steel/steel	3 mm	2.0 N	0.81 GPa

Thus, SRR = 0% (i.e. $u_{ball} = u_{disk}$) represents a pure rolling contact and SRR = 200% (i.e. either u_{ball} or $u_{disk} = 0$) represents a pure sliding contact, while the values between 0 and 200% represent a mixed sliding/rolling contact. With the given software (PCS Instruments, MTM version 1.0), values of 1 to 200% of SRR were accessible. Under a given SRR, the coefficient of friction (dF/dN) is measured as a function of *mean* velocity. To investigate the lubrication behaviors of the polymers at different slide/roll ratios, the coefficient of friction versus mean velocity plots were obtained at different SRRs.

All the friction measurements were performed under a fixed load (3.0 or 20.0 N) and temperature (25 °C) and along the same ball and disk tracks; the radii of the ball and disk tracks are 9.5 and 20.7 mm, respectively. The roughness values (R_a) of the ball and disk are 11 and 10 nm respectively. However, different pairs of the ball/disk tracks were used for the comparison of the friction measurement in the absence versus presence of the polymers in buffer solution, due to significant wear of the tribo-pair in the former case. The calculated maximum contact pressures are 0.86 and 0.46 GPa for 20.0 and 3.0 N, respectively (see table 1).

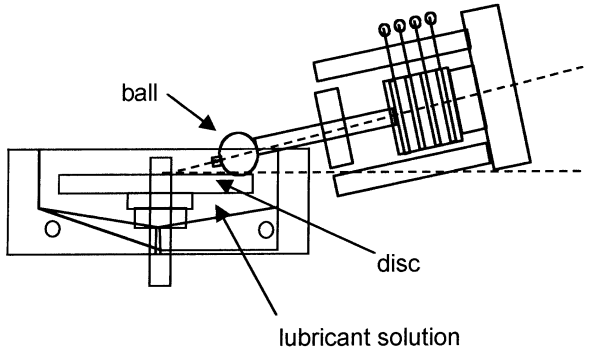

Figure 3. A schematic set-up of the mini traction machine (MTM).

2.5. Pin-on-disk tribometry

A pin-on-disk tribometer (CSM, Neuchâtel, Switzerland) was employed to characterize the friction and lubrication properties of aqueous PLL(10)-*g*[2.9]-PEG(2) solutions in the pure sliding contact regime. In this set-up, a fixed, spherical steel ball (6 mm in diameter, DIN 17 230, Hydrel, Romanshorn, Switzerland) is in contact with a flat disk. Both glass (SuperFrost, soda-glass, Menzel-Gläser, Braunschweig, Germany) and steel (DIN 17 230, XXX, Switzerland) were selected for the disk, thus representing the FeO_x/SiO_x and FeO_x/FeO_x pairings. The roughness values (R_a) for steel ball, steel disk, and glass disk are 32, 5, and 5 nm respectively. The load was controlled by placing dead weights on top of the ball holder (0.5 to 5.0 N) and the friction forces were measured by a strain gauge. The friction signals were recorded with a Macintosh Power PC using Labview and an ADC card of the MIO family (both from National Instruments, Austin, TX, USA). To investigate the lubricating properties of the polymer, both load and velocity dependence of the frictional properties were explored. For each friction measurement, different fresh tracks were selected. For this reason, the comparison of the frictional properties with or without polymers could be performed with exactly the same set-up of the tribo-pair. All the measurements were performed at room temperature (~25 °C). The calculated maximum contact pressures are presented in table 1.

2.6. Cleaning of the tribo-pairs

All the instrumental parts that are expected to be coated with the polymer, including the waveguides for the OWLS and the balls/disks of all tribological instruments, were oxygen-plasma cleaned for ca. 2 min in a Harrick Plasma Cleaner/Sterilizer PDC-32G

instrument (Ossining, NY, USA) prior to the measurements. Before the plasma cleaning, the instrumental parts were rinsed with copious amounts of water or organic solvents as follows: The waveguides of the OWLS were sonicated in 0.1 M HCl for 10 min, extensively rinsed with ultra-high-purity water, and dried under nitrogen; the ball/disk and the assembly parts of ultra-thin film interferometry and MTM were degreased by sonication in toluene for 10 min, followed by sonication in iso-propanol for 10 min, and subsequently dried under nitrogen; the balls and disks of pin-on-disk and assembly parts were sonicated in ethanol for 10 min and dried under nitrogen.

3. Results and discussion

3.1. Adsorption behavior of PLL(10)-g[2.9]-PEG(2) on silicon oxide and iron oxide substrates

In figure 4, representative OWLS adsorption measurements for the PLL(10)-*g*[2.9]-PEG(2) on (a) silicon oxide and (b) iron oxide are presented. All measurements were carried out *in situ* in a flow-through cell without an intermittent drying stage.

As expected, the results of OWLS experiments indicate that the PLL(10)-*g*[2.9]-PEG(2) spontaneously adsorbed from a pH 7.4 HEPES (10 mM) buffered aqueous solution (0.25 mg/ml) onto both oxide surfaces. A PLL-*g*-PEG layer of areal density of approximately 120 ng/cm^2 and 60 ng/cm^2 was formed on silicon oxide and iron oxide, respectively. The difference in areal density for the two substrates is understood by considering the difference in IEPs of the two oxide substrates and thus the corresponding differences in charge density at a given pH. In previous studies involving several other metal oxides, a lower IEP for a given substrate has been correlated with a higher areal density of PLL-*g*-PEG [22,23]. The lower IEP of silicon oxide (~ 2) when compared with iron oxide (6–9) is consistent with the higher areal density of PLL-*g*-PEG adsorbed on the silicon oxide. In both cases, 95% of the final mass was reached within the first 5 min. There was no apparent desorption following rinsing with buffer solution on the timescale of the experiment. All tribological experiments involving the polymers were carried out 30 min after the tribo-pair was immersed in polymer-containing solution, to ensure adequate time for adsorption.

As described in the experimental section, the tribo-pairs used in this work were prepared in different ways from the substrates (waveguides) used in the OWLS experiment, although all are either silicon oxide- or iron oxide-based materials. It is thus noted that the actual amount of the adsorbed polymers on each tribo-pair may be slightly different from those shown in figure 4.

3.2. Lubrication properties in rolling contact

The lubrication properties of the PLL(10)-*g*[2.9]-PEG(2) were characterized under pure rolling contact conditions by employing ultra-thin-film interferometry. In contrast to the other tribological approaches in this work, which determine the interfacial friction forces, ultra-thin film interferometry uniquely measures the film thickness of a lubricated contact. In this work, the film-thickness measurements were first performed under polymer-free buffer solution. No meaningful data were obtained, due to significant wear of the contact in this condition. Only in a high-velocity regime (> 1000 mm/s) has an interfacial film involving pure water as a lubricant been reported [8]. However, following addition of the polymers to the buffer solution, the measurement of the lubricant-film thickness was reproducibly achieved over a wide range of

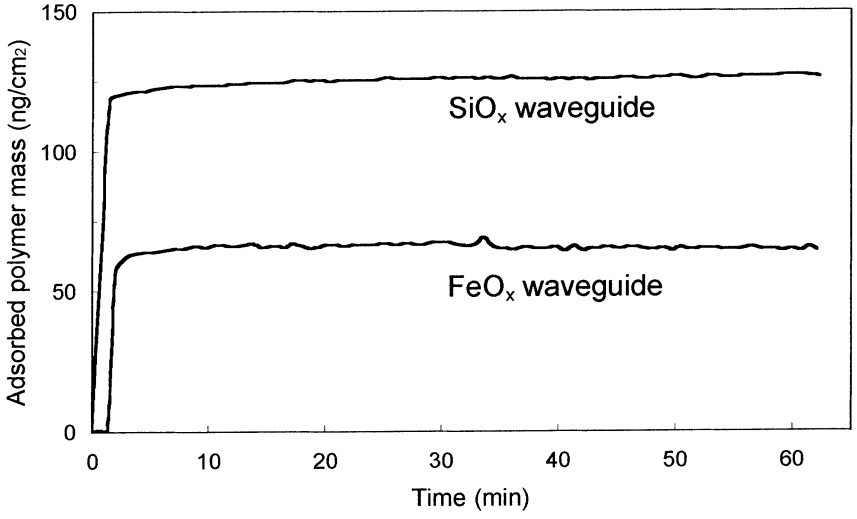

Figure 4. Representative adsorption profiles of PLL(10)-*g*[2.9]-PEG(2) onto (a) silicon oxide and (b) iron oxide substrates as measured by OWLS (buffer solution = 10 mM HEPES (pH 7.4), concentration of the polymer = 0.25 mg/ml; T = 25 °C).

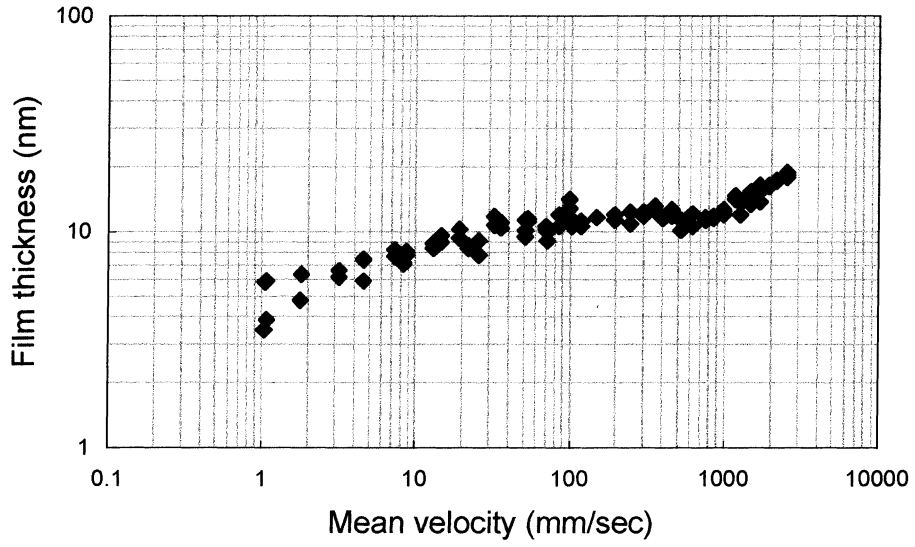

Figure 5. Log (film thickness) versus log (velocity) plot by ultra-thin-film interferometery (ball = AISI 52100 steel (19 mm in diameter), disk surface = sputtered silica, buffer solution = 10 mM HEPES (pH 7.4), concentration of the polymers = 0.25 mg/ml, load = 20.0 N, T = 25 °C).

velocities. The results are shown as a log (film thickness) versus log (velocity) plot in figure 5.

The lubricant-film formation in the presence of the polymer in figure 5 exhibits three velocity regimes: (i) velocity range lower than ~30 mm/s, where the film thickness gradually decreases with decreasing velocity, (ii) velocity range from ~30 to ~1000 mm/s, where the measured film thickness is nearly constant (thickness 11.4 ± 1.0 nm in average), and (iii) velocity range higher than ~1000 mm/s, where the film thickness increases with increasing velocity (slope ~0.4 in log–log plot). The nearly constant film thickness obtained over a wide range of velocities (~30 to 1000 mm/s) suggests that a boundary-layer-lubrication mechanism is active in this regime. The high-velocity region where film thickness increases with increasing velocity is similar to that previously observed for pure water and probably represents the hydrodynamic entrainment of water into the contact. The velocity-dependent behavior of the lubricant-film thickness for the PLL(10)-*g*[2.9]-PEG(2)-containing buffer solution in the low-velocity regime is qualitatively similar to that of surfactant (sodium olefin (C16) sulfonate)-containing water, reported in a previous study [8]. However, a relatively thicker layer is observed in this work (~ 11 nm versus ~3 nm), attributed to the brush-like structure of this polymer.

3.3. Lubrication properties in mixed sliding/rolling contact

The lubrication properties of PLL(10)-*g*[2.9]-PEG(2) solutions have been characterized in a mixed sliding/rolling contact regime by means of MTM. As described in the experimental section, a mixed sliding/rolling contact was achieved by independent driving of the ball and disk, to form a lubricated contact. In this work, the measurement was initially performed under 20.0 N load. Regardless of the slide/rolling ratio, the friction forces were very high and irreproducible. Furthermore, no noticeable reduction of friction forces was observed by addition of the polymers into buffer solution, which is in contrast to the results shown in section 3.2. This may be due partly to the higher contact pressure for the FeO_x/FeO_x pair (max. 0.86 GPa) compared to the FeO_x/SiO_x pair (max. 0.51 GPa), and partly to the lower areal density of PLL-*g*-PEG on the iron oxide surface, as measured by OWLS in section 3.1. Thus, the measurements were carried out under a lower-pressure regime by applying a load of 3.0 N (max. 0.46 GPa). The coefficient of friction was measured as a function of velocity at three different slide/roll ratios, SRR = 50 and 100% for comparison. Due to an instrumental resolution issue, measurements were only able to be made in the velocity range shown in figure 6.

For SRR = 50%, apparently higher values of friction were observed in pure buffer solution than the polymer-containing solution. Furthermore, monotonically decreasing frictional properties (from $\mu = 0.43$ to $\mu = 0.22$) as a function of increasing velocity were observed. The polymer-containing solution, on the other hand, showed similar velocity-dependent frictional behavior, but with clearly lower coefficients of friction ($\mu = 0.25$ to $\mu = 0.12$) within the same velocity range. The frictional properties at SRR = 100% were observed to be similar to those at SRR = 50%. The coefficient of friction reduced from 0.42 to 0.26 in buffer solution to 0.26 to 0.09 in the presence of the polymers. It is noted that all measurements were performed on the same disk track, although different balls and disks were used for measurements with or without polymers.

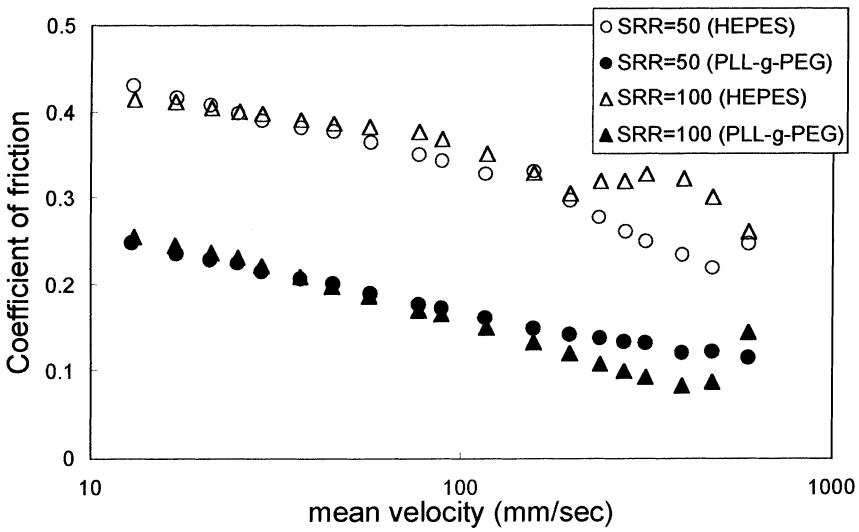

Figure 6. Log (coefficient of friction) versus log (velocity) plot by MTM slide/roll ratio (SRR) = 50% and 100%. Empty symbols are for buffer solution only and filled symbols are for the polymer in buffer solution (ball = AISI 52100 steel (17.4 mm in diameter), substrate = AISI 52100 steel, buffer solution = 10 mM HEPES (pH 7.4), concentration of the polymer = 0.25 mg/ml, load = 3.0 N, T = 25 °C).

Due to the relatively narrow range of velocities available, it is not trivial to determine what lubrication regime is activated for the mixed sliding/rolling contact in this work. However, the results above show that the PLL(10)-*g*[2.9]-PEG(2) can effectively reduce the frictional properties at mixed sliding/rolling contact of FeO_x/FeO_x in buffer solution.

3.4. Lubrication properties in sliding contact

Finally, the lubrication properties of the PLL(10)-*g*[2.9]-PEG(2) were characterized in a pure sliding-contact regime by employing pin-on-disk tribometry. Stainless steel was selected as ball and both glass and steel were selected as disks. The lubrication properties of the PLL(10)-*g*[2.9]-PEG(2) were investigated by comparing the frictional properties of the tribo-pair in the presence and absence of the polymers in buffer solution. In this experiment, the lubrication properties of PLL(10) were also included for comparison.

Firstly, the load dependence of the frictional properties for the steel/glass tribo-pair was investigated. In this experiment, the friction forces were measured on fresh tracks for each load (0.5 to 5.0 N), while keeping the rpm constant and the total number of revolutions below 5. The resultant velocity was within the range of ~ 0.2 to ~ 0.8 mm/s, which is close to the lowest value achieved with the tribometer. As will be shown below, the frictional properties were virtually independent of the slight variation of the velocity in that range. The results are shown in figure 7. In all cases, the frictional forces are fairly linear with increasing applied load. It is also noticeable that the friction forces of the steel/glass pair are significantly reduced by addition of the polymers into the buffer solution. The coefficient of friction of the steel/glass tribo-pair, obtained by taking the slope of friction versus load plots ($\Delta F/\Delta L$ (L = 0.5 to 5.0 N)) decreased from 0.34 to 0.15 by the addition of PLL(10), and further decreased to 0.09 by the addition of PLL(10)-*g*-[2.9]-PEG(2).

Secondly, the velocity dependence of the frictional properties for the steel/glass tribo-pair was investigated. For this experiment, the friction forces were also measured on fresh tracks for each velocity in the range of ~ 0.1 to ~ 400 mm/s. All the measurements were performed under a fixed load (2.0 N) and the total number of revolutions was extended to 100. The results are shown in figure 8. The friction versus velocity plots in figure 8 reveal that there are two distinct velocity regimes in which the frictional properties of the tribo-pair in the presence versus absence of the polymers in buffer solution can be compared. In the velocity regime lower than ~40 mm/s, the frictional properties of the tribo-pair can clearly be distinguished in magnitude in decreasing order, *buffer solution only* $\geq$ *PLL(10)* > *PLL(10)-g[2.9]-PEG(2)*, which is consistent with the load-dependent frictional properties shown in figure 7. In the velocity regime higher than ~40 mm/s, however, the difference between the lubricants diminishes and the frictional properties of the tribo-pair in buffer solution is not significantly influenced by the presence of the polymers. Throughout the entire velocity range, the sliding of the tribo-pair in the presence of buffer solution only or with PLL(10) appears to decrease with an increase of the velocity. Meanwhile, the corresponding sliding in the presence of PLL(10)-*g*[2.9]-PEG(2) appears to exhibit a virtually constant coefficient of friction (0.062 ± 0.019 on average). This is highly indicative of boundary-layer formation by the PLL(10)-*g*[2.9]-PEG(2) on these oxide surfaces in aqueous buffer solution. For both load- and velocity-

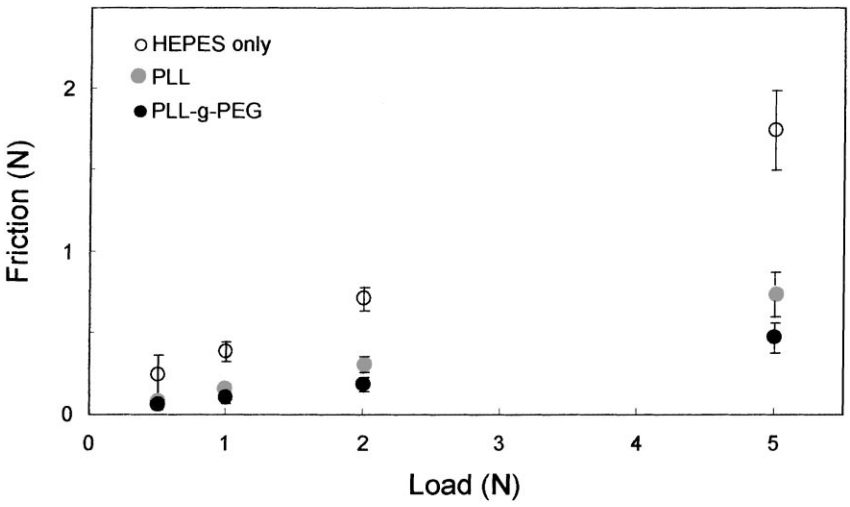

Figure 7. Friction force versus load plot (pin-on-disk tribometer) of buffer solution only (○), PLL(10) in buffer solution (◍), and PLL(10)-*g*[2.9]-PEG(2) in buffer solution (●) (ball = steel (6 mm in diameter), disk = glass, buffer solution = 10 mM HEPES (pH 7.4), concentration of the polymer = 0.25 mg/ml, load = 0.5 − 5.0 N, T = 25 °C).

dependence measurements, it appears that the lower frictional properties of the PLL(10)-*g*[2.9]-PEG(2) compared with PLL(10) indicate a significant role of the brush-like PEG side chains in lubrication of the tribo-interfaces, as suggested in studies on end-grafted polymers in organic solvents [12–18].

Finally, the load and velocity dependence for pure sliding of the FeO_x/FeO_x tribo-pair has been investigated. The coefficient of friction obtained from the slope of the friction versus load plots ($\Delta F/\Delta L$ (L = 0.5 to 5.0 N)) after 5 rotations decreased from 0.30 to 0.14 upon addition of polymer. However, the coefficient of friction, dF/dN (N = 2.0 N) that was obtained after 100 rotations for each velocity, which remained virtually constant over the range of ~1 to ~ 100 mm/s, was not significantly reduced upon addition of polymer ($\mu = 0.31 \pm 0.05$ without polymer to $\mu = 0.27 \pm 0.03$ with polymer on average). The reduced lubrication effect of PLL(10)-*g*[2.9]-PEG(2) for the sliding of a FeO_x/FeO_x tribo-pair (with respect to FeO_x/SiO_x tribo-pair) is thought to be mainly correlated with the relatively lower amount of polymer adsorption (see figure 4).

4. Summary

The lubrication properties of PLL(10)-*g*[2.9]-PEG(2) (PLL-*g*-PEG) as an additive for tribo-systems composed of silicon oxide and iron oxide in an aqueous environment have been characterized employing several macroscopic tribological approaches. The tribological properties of tribo-pairs lubricated by a PLL-*g*-PEG-containing aqueous buffer solution have been investigated in various dynamic contact regimes encountered

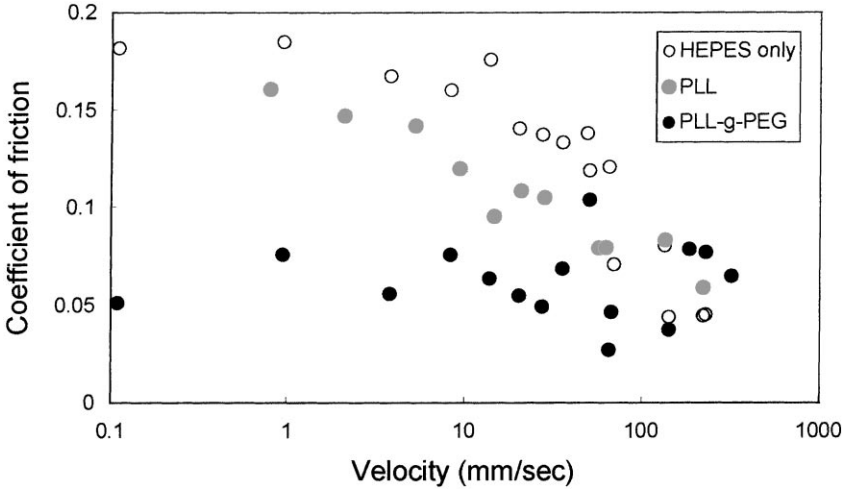

Figure 8. Log (coefficient of friction) versus log (velocity) plot by pin-on-disk tribometer of buffer solution only (○), PLL(10) in buffer solution (◍), and PLL(10)-*g*[2.9]-PEG(2) in buffer solution (●) (ball = steel (6 mm in diameter), disk = glass, buffer solution = 10 mM HEPES (pH 7.4), concentration of the polymer = 0.25 mg/ml, load = 2.0 N, T = 25 °C). In this plot, the error bars, typically 0.05 for buffer solution only and 0.02 for the polymers, are omitted for clarity.

in engineering systems: (1) pure rolling contact of a FeO_x/SiO_x tribo-pair, as measured by ultra-thin film interferometry, showed that the polymer-containing buffer solution forms a stable lubricant film (11.4±1.0 nm on average) over a wide velocity range (~ 30 to 1000 mm/s); (2) the mixed sliding/rolling contact of an FeO_x/FeO_x tribo-pair measured by MTM showed that the friction forces were reduced by approximately one-half upon addition of PLL-*g*-PEG when the slide/roll ratio is 50 or 100% in a low-pressure regime; (3) pure sliding contact of an FeO_x/SiO_x tribo-pair, measured by a pin-on-disk tribometer, showed a significant reduction of friction (remains constant at 0.06±0.019 on average for ~ 0.1 to 400 mm/s), while less effective lubrication was observed upon the sliding contact of an FeO_x/FeO_x tribo-pair.

The effectiveness of boundary lubrication by PLL(10)-*g*[2.9]-PEG(2) in aqueous buffer solution is very apparent in relatively low velocity regimes, where lubrication by water alone is practically impossible due to its extremely low pressure-coefficient of viscosity and poor film-forming properties. The relative adsorption behavior of the polymer onto SiO_x and FeO_x surfaces, as investigated by OWLS (~ 120 ng/cm^2 for SiO_x and ~ 60 ng/cm^2 for FeO_x surfaces), seems to explain the relatively less effective lubrication for FeO_x/FeO_x compared with the FeO_x/SiO_x tribo-pair. In summary, the PLL(10)-*g*[2.9]-PEG(2) appears to form a protective layer both on silicon oxide and iron oxide surfaces, thus effectively improving load-carrying and boundary lubrication properties of water for a variety of dynamic contact regimes.

Acknowledgments

This work was financially supported by the Council of the Swiss Federal Institutes of Technology (ETH-Rat TopNano 21) and National Research Program 47 of the Swiss National Science Foundation. We are also grateful to Dr. Philippa Cann and Ms. Ksenia Toplovec Miklozic of Imperial College for their valuable advice and assistance, as well as Michael Horisberger (Paul Scherrer Institute, Villigen, Switzerland) for the sputter coating.

References

[1] G.D. Jay, K. Haberstroh and C.-J. Cha, J. Biomed. Mat. Res. 40 (1998) 414.
[2] I.M. Schwarz and B.A. Hills, British J. Rheum. 37 (1998) 21.
[3] B.A. Hills, Proc. Instrn. Mech. Engrs. 214 (2000) 83.
[4] M. Scherge and S.N. Gorb, *Biological Micro- and Nano-tribology* (Springer, Berlin, 2001).
[5] M. Ratoi-Salagean, H.A. Spikes and R. Higendoorn, Proc. Instrn. Mech. Engrs. 211 (1997) 195.
[6] M. Ratoi-Salagean, H.A. Spikes and H.L. Rieffe, Tribol. Trans. 40 (1997) 569.
[7] S.R. Schmid and W.R.D. Wilson, Lub. Eng. 52 (1995) 168.
[8] M. Ratoi-Salagean and H.A. Spikes, Tribol. Trans. 42 (1999) 479.
[9] S. Plaza, L. Margielewski, G. Celichowski, R.W. Wesolowski and R. Stanecka, Wear 249 (2001) 1077.
[10] S. Hollinger, J.-M. Georges, D. Mazuyer, G. Lorentz, O. Aguerre and N. Du, Tribol. Lett. 9 (2000) 143.
[11] B. Duan and H. Lei, Wear 249 (2001) 528.
[12] J. Klein, Annu. Rev. Mater. Sci. 26 (1996) 581.
[13] J. Klein, E. Kumacheva, D. Perahia and L.J. Fetters, Acta Polym. 49 (1998) 617.
[14] U. Raviv, R. Tadmor and J. Klein J. Phys. Chem. B. 105 (2001) 8125.
[15] S. Granick, A.L. Demirel, L.L. Cai and J. Peanasky, Isr. J. Chem. 35 (1995) 75.
[16] J. Klein, D. Peraha and S. Warburg, Nature 352 (1991) 143.
[17] G.S. Grest, Phys. Rev. Lett. 76 (1996) 4979.
[18] T. Kreer, M.H. Müser, K. Binder and J. Klein, Langmuir 17 (2001) 7804.
[19] A.S. Sawhney and J.A. Hubbell, Biomaterials 13 (1992) 863.
[20] D.L. Elbert and J.A. Hubbell, Chem. Biol. 5 (1998) 177.
[21] D.L. Elbert and J.A. Hubbell, J. Biomed. Mater. Res. 42 (1998) 55.
[22] G.L. Kenausis, J. Vörös, D.L. Elbert, N.-P. Huang, R. Hofer, L. Ruiz-Taylor, M. Textor, J.A. Hubbell and N.D. Spencer, J. Phys. Chem. B 104 (2000) 3298.
[23] N.-P. Huang, R. Michel, J. Vörös, M. Textor, R. Hofer, A. Rossi, D.L. Elbert, J.A. Hubbell and N.D. Spencer, Langmuir 17 (2001) 489.
[24] G.A. Parks, Chem. Rev. 65 (1965) 177.
[25] R. Kurrat, M. Textor, J. J. Ramsden, P. Böni and N.D. Spencer, Rev. Sci. Instrum. 68 (1997) 2172.
[26] R. Kurrat, B. Walivaara, A. Marti, M. Textor, P. Tengvall, J. J. Ramsden and N.D. Spencer, Colloids Surf. B 11 (1998) 187.
[27] J. Vörös, J.J. Ramsden, G. Csucs, I. Szendrö, S.M. De Paul, M. Textor and N.D. Spencer, Biomaterials 23 (2002) 3699.
[28] J.J. Ramsden, J. Stat. Phys. 73 (1993) 853.
[29] G.J. Johnston, R. Wayte and H.A. Spikes, Tribol. Trans. 34 (1991) 187.
[30] G.R. Paul and A. Cameron, Proc. Roy. Soc. Lond. A331 (1972) 171.
[31] M. Smeeth and H.A. Spikes, J. Tribol. 119 (1997) 291.
[32] T.H. Courtney, *Mechanical Behavior of Materials*, 2nd ed. (McGraw-Hill/Higher Education, International Edition, 2000).